Federal Agency: National Institute of Justice
Federal Grant of Identifying Number Assigned by Agency: 903892261 (Sponsor)
Project Title: Post-mortem changes and translocation of bacterial community structure and function for use in criminal investigations
PD/PI Name: Heather R. Jordan
Title: Assistant Professor
Contact Information: Jordan@biology.msstate.edu; hwillia8@gmail.com (secondary); 662-325-8252
Name of Submitting Official: Heather R. Jordan
Submission Date: 08-31-2018
DUNS Number:
EIN Number:
Recipient's Organization: Mississippi State University
Recipient Address: 449 Hardy Road, 133 Etheredge Hall, Mississippi State, MS 39759
Recipient Identifying Number or Account Number: 2014-DN-BX-K008
Project/Grant Period: 01/01/2015-08/31-2018
Report Term: Final Summary Overview
Signature of Submitting Official: Heather R. Jordan

Project Overview

Determination of the post-mortem interval is a critical measure following events of homicide or un-witnessed deaths, and resolving the precise window of time and location of both the decedent and witness(es) is essential for excluding or including witnesses, and unlocking circumstances leading to death. However, there are challenges with reliability and accuracy in describing the post-mortem interval (PMI). While there are recognizable changes that a body undergoes during decomposition, there are key variables that advance and retard the rate of these processes. Some significant factors include environmental conditions, body habitus, predation, external microbiota, and microbes resident to the human body, known as the microbiome.

In a first-of-its-kind effort, we sought to expand studies of the post-mortem microbiome by partnering with a major, metropolitan city's medical examiner's office to sample and analyze, using next-generation sequencing and imaging technology, bacterial communities from anatomical locations of human cadavers to maximize demographic sampling and representation,

several different manners of death, and confirmed PMIs. In another novel series of transformative controlled laboratory studies using fluorescently labeled bacteria in vertebrate models, we described how the microbiome of a living host changes and translocates within the body after death – linking the microbiome of a living being to the post-mortem microbiome changes, which have demonstrated such promise as usable evidence in criminal investigations.

The major goals of this project were to:

1. Use a large sample size of human cadavers from routine death investigations to evaluate the importance and variability of the post-mortem human microbiome.
2. Describe how the microbiome of a living host changes and translocates within the body after death.

The objectives of this project were to:

1. Describe human epinecrotic bacterial communities (structure) and their functional gene potential on different areas of the body in relation to sex, race, manner of death, geographic location of the body recovery, and autopsy confirmed PMIs.
2. Determine bacterial structure, functional potential and translocation (migration or dispersal) within the body during the course of decomposition.

Goal One, Objective One. For the first goal, and for objective one, we coordinated with the Wayne County Medical Examiner's Office Chief Medical Examiner, Dr. Carl Schmidt (Detroit, MI metropolitan area), to obtain swab samples of the auditory canal, nose, mouth rectum, umbilicus and bone marrow (at autopsy) from human cadavers taken from routine death investigations and at autopsy. For the project period, we were able to collect swabs from over 1,500 individuals. Of those, we have isolated DNA, quantified, sequenced and analyzed the bacterial communities of swabs from approximately 240 individuals. Several major products have resulted from this work that will be summarized below.

Study One-Frozen: Thawing and Its Effect on the Post-mortem Microbiome in Two Pediatric Cases.

Details of this study can be found in Pechal, et al, *J. Forensic Sci*, 2017. Briefly, post-mortem microbiome analyses were conducted, corresponding with autopsy investigation of unusual pediatric cases where bodies were found substantially altered due to long-term freezing and concealment for two different timepoints. Microbial swab samples were aseptically collected at three time points during the thawing process: when completely frozen and immediately after extraction from the freezer, partially thawed (*c*. 24 h post-discovery), and when fully thawed (*c*. 48 h post-discovery) for autopsy. The microbial communities were sampled from six external anatomic locations at each time period during the thawing: the external auditory canal, eyes, nares, mouth, umbilicus, and rectum. Results showed freezing artifacts from all tissues. Furthermore, microbiome data demonstrated that the post-mortem human microbiome changes during the thawing of frozen individuals. The study also provided microbiome data from an unusual case that may be useful for estimating long-term post-mortem intervals that result from concealing a body in ways that slow or limit decomposition and subsequent microbial activity.

Study Two- A large-scale survey of the post-mortem human microbiome, and its potential to provide insight into the living health condition. Details of this study can be found in Pechal, et al, *Scientific Reports*, 2018. For this study, we used targeted 16s rRNA gene amplicon sequencing to analyze microbial taxa collected from swab sample DNA from 188 human cases representing a cross-section of an industrial-urban population. We explored relative abundance of prominent genera associated with anatomical location and PMI. From this NIJ supported work,

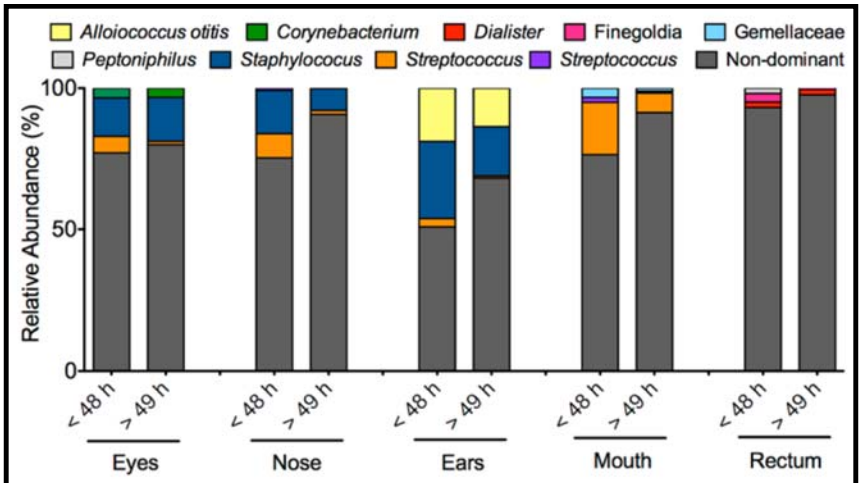

Figure 1. Relative abundance of prominent microbial genera associated with anatomical locations and PMI, from 188 human bodies.

we identified prominent genera driving PMI (Figure 1). Results showed that *Staphylococcus*, *Streptococcus, and Finegoldia* were among the most dominant identified commensal genera across eyes, nose, and rectum swab samples, with modulation of relative abundance across decomposition time.

We also tested whether predicted functional community profiles shifted during decomposition. For this, we explored the inferred KEGG ortholog pathways and identified significant functional signatures that varied with post-mortem interval. Using machine-learning models, we found anatomic areas, except the rectum, showed model accuracy and areas under the curves in the receiver operating characteristic (ROC) plots being near. Models showed an observed increase in cell motility pathways, including chemotaxis, motility proteins, and flagellar assembly 48H or greater post-mortem, most notably in the mouth (Figure 2).

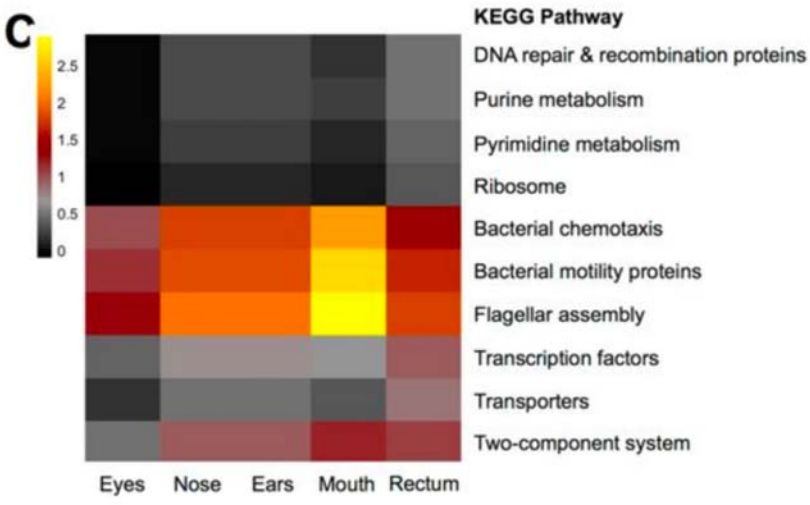

Figure 2. Microbial KEGG orthology pathways detected in anatomical locations of bodies >48H post-mortem.

This resource was prepared by the author(s) using Federal funds provided by the U.S. Department of Justice. Opinions or points of view expressed are those of the author(s) and do not necessarily reflect the official position or policies of the U.S. Department of Justice.

Finally, we performed a power analysis for the post-mortem microbiome. We computed the power of detecting a community shift for two groups of unequal sample size for each anatomic location at a significance level of 5%. Our results indicated samples from the mouth had the greatest discriminating power (Cohen's d = 1.13; power = 1). Power analyses showed that a large-scale study, such as ours, is necessary for characterizing post-mortem microbiome changes.

Study 3-Human Microbiome Shotgun Metagenomic Sequencing Results *(Data presented here are currently in submission to JAMA open access)*. Shotgun metagenomics sequencing was conducted on samples from the trabecular space or interhemorrhagic fissure of 31 human bodies. Community analysis showed diversity across all bodies (Figure 3A). Additionally, functional prediction conducted against a variety of ante-mortem metrics identified significant functional markers for race identification among bodies assayed (Figure 3B, white, light blue; black, red). We next conducted gene finding targeted for antibiotic resistance genes (AbxR) among 16 of the samples in an effort to determine baseline AbxR within the study population. Results showed AbxR genes detected in all bodies, but with variability with regard to number, AbxR classes, and year (Figure 3C and D). Results of this in-depth, global screening underscore the potential of these methods to relate microbial community and genetic signatures to body attributes. Furthermore, our methods for gene finding have promising utility for detection

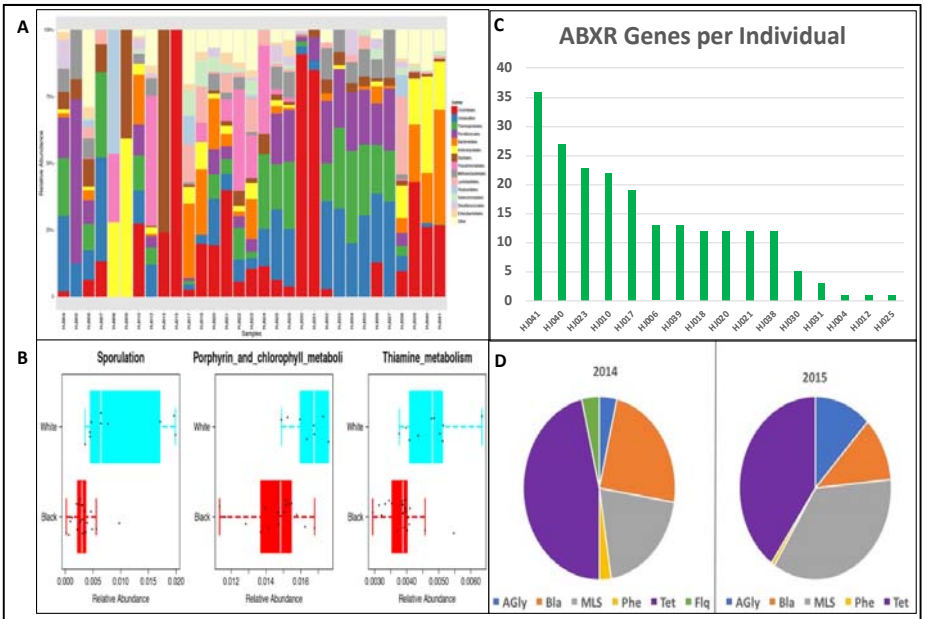

Figure 3. Results from shtogun metagenomic sequencing and analysis of trabecular space and interhamorrhagic fissure samples collected from bodies. A. Community analyses showed diversity across samples (class level). B. Functional profiling found significant genetic markers distinguishing race. C. Gene finding for antibiotic resistance (ABXR) identified many ABXR genes within the sample set with differening abundance across sampling years (D).

and prediction of disease outbreaks and determination of baseline and epidemic gene levels among human populations for microbial source tracking and surveillance.

Goal Two, Objective Two. To meet the second goal and objective two, we utilized an animal model for the study of microbial translocation and functional potential following host death. We designed a study where fluorescently labeled bacteria were inoculated into mice and tracked through whole body imaging following host death. For our studies, *Staphylococcus aureus*-RFP and *Clostridium perfringens* type A were introduced intranasally or orally through gavage to SKH-1 hairless, immunocompetent Elite female mice and sacrificed 24 hours after inoculation. Thirty mice were surface sterilized by submersion in a bleach solution to determine impact of external microflora. All mice were placed individually in sterile containers allowing filtered airflow during decomposition and allowed to remain until designated post-mortem timepoint analyses. Three mice per treatment were dissected per time point and all organs and bone marrow were subjected to whole body imaging, nucleic acid isolation for culture, qPCR targeting RFP, whole genome shotgun metagenomics and shotgun metatranscriptomics.

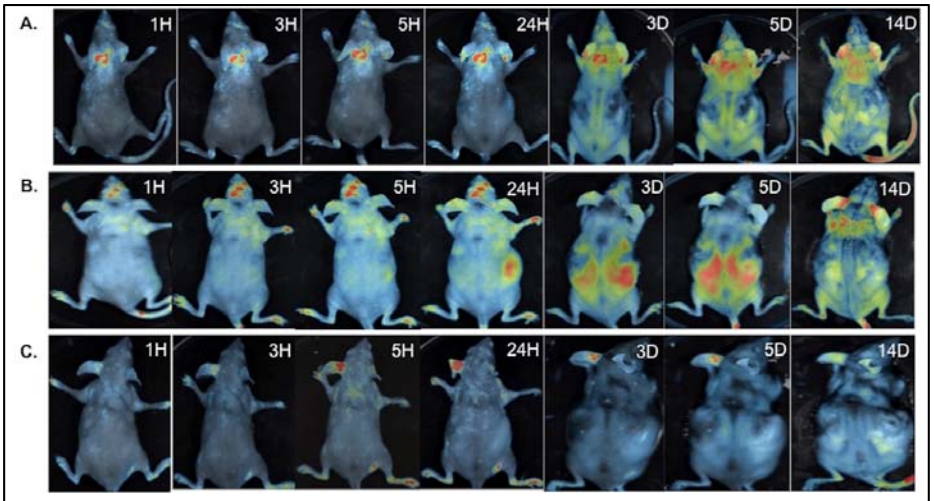

Figure 4. Whole body imaging using iBox Scientia (UVP) detecting Staphylococcus aureus KUB7 translocation in infected, surface sterilized (A), infected, non-surface sterilized (B) and uninfected, control mice (C), 3H, 5h, 24H, 3D, 5D, and 14D post-mortem. The intensity of fluorescence is based on a scale from blue being the lowest and red being the highest.

Whole body fluorescent imaging showed *S. aureus*-RFP transmigration across decomposition time. Whole body fluorescent imaging showed *S. aureus*-RFP nasal colonization 1H post sacrifice in the surface sterilized and non-surface sterilized mice (Figure 4, panels A and

B). Imaging showed evidence of increased *S. aureus* KUB7 transmigration occurring in the non-surface sterilized mice over decomposition time. *S. aureus* KUB7 was at the highest detectable concentrations within the nasopharyngeal area among surface sterilized mice up to 24H, but was detected throughout the body among non-surface sterilized mice during this timeframe. Increased visible evidence of transmigration was found from 3D to 14D in both sample sets.

Representative qPCR and microbial community data are shown for intranasally infected mice for timepoints one hour (1H) through seven days (7D) (Figure 5, Panels A and B, Burcham, et al, *In preparation*) for bone marrow (Figure 5A) and heart (Figure 5B) samples. *S. aureus*-RFP was detected in bone marrow within the first hour PMI timepoint, that decreased at 3H, but increased over time to the 7D timepoint (Figure 5A). *S. aureus*-RFP was not detected in heart samples until the 7D PMI timepoint (Figure 5B).

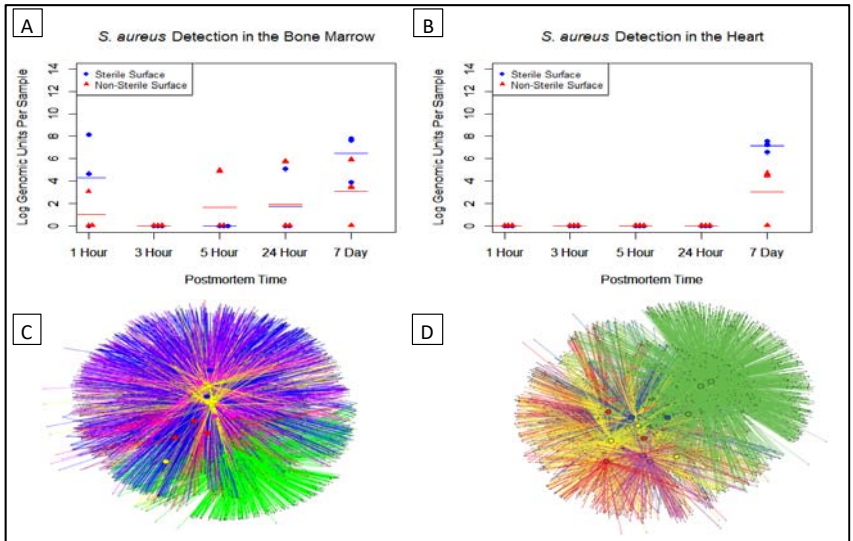

Figure 5: Quantitative PCR (A and B) and network analysis of microbial community data (C and D) results in bone marrow (A and C), and heart samples (B and D) from *S. aureus*-RFP nasally infected mice. qPCR results show quantitation from surface sterilized (blue) versus non-surface sterilized (red) mice.

Shotgun metagenome sequences from organs across decomposition time were trimmed using Trimmomatic to remove nucleotides with an average phred 33 score less than 28, and read lengths less than 36bp. Trimmed reads were used to determine bacterial genera relative abundance in each sample using MetaPhlAn2. Network analyses of bone marrow (Figure 5C) and heart (Figure 5D) showed similar patterns where operational taxonomic units (OTUs) were not clearly defined overall across PMI in early timepoints of 1H, 3H, 5H, and 24H (line colors: blue, pink, red, respectively). However, OTUs clustered together at the 7D timepoint (green lines).

Bray-Curtis distances were calculated and transformed, and a constrained distance-based redundancy analysis (db-RDA) was determined using the forward selection of the explanatory variables (PMI, organ, colonized, sterilized, treatment) based on adjusted R^2 and p-value. The best model was with PMI (adj. R^2=0.18, p=0.002) and organ (*adj.* R^2=0.32, p=0.002). A PMI:Organ dbRDA ordination plot was created including genera that showed a significant environmental fit by linear combination scores (Figure 6). From the dbRDA plot, *Staphylococcus* and *Parabacteroides* explained most of the variation associated with PMI<24H within the bone marrow and intestine samples, respectively (R^2=.35; p=0.002 and R^2=.65; p=0.001, respectively). *Clostridium* explained most of the variation at 7D within all organ DNA samples (R^2=0.76; p=0.001).

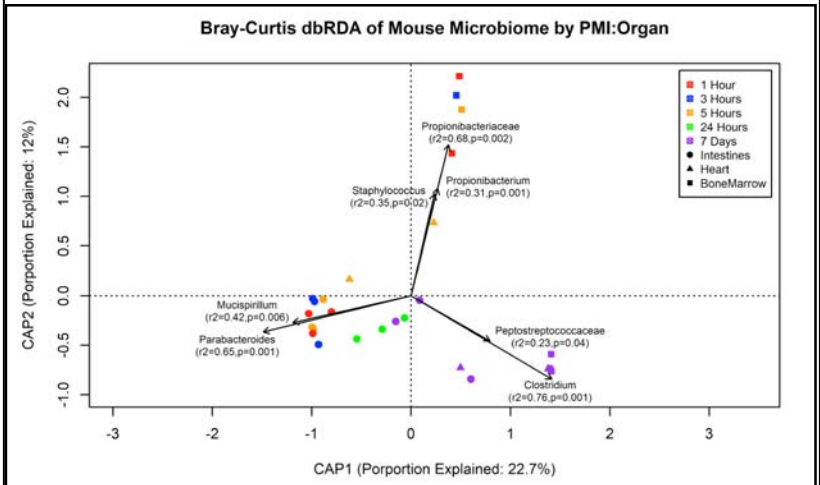

Figure 6. PMI: Organ Distance-based redundancy analysis ordination plot including genera showing significant environmental fit by linear combination scores.

Results from orally infected mice are shown in Figure 7. Visualization of the weighted and unweighted UniFrac distances with a PCoA (Figure 7) showed that the heart and bone marrow, then intestines and stomach tended to group closely. In the weighted UniFrac PCoA (Figure 7A), the ≤26h heart and bone marrow all clustered closely and the ≤26h intestines clustered together but separate from the heart and bone marrow. Interestingly, the ≤26h stomach samples had a larger variability between them, but continued to stay in the range of the other ≤26h timepoints. As decomposition progressed to 170h post-mortem, the intestines and stomach became similar, likely due to the samples being dominated by Lactobacillaceae and the heart and bone marrow likely became similar with the increase of Clostridiaceae I. Samples primary moved along axis 1 as decomposition progresses which explains 49% of the variation. The heart and bone marrow

This resource was prepared by the author(s) using Federal funds provided by the U.S. Department of Justice. Opinions or points of view expressed are those of the author(s) and do not necessarily reflect the official position or policies of the U.S. Department of Justice.

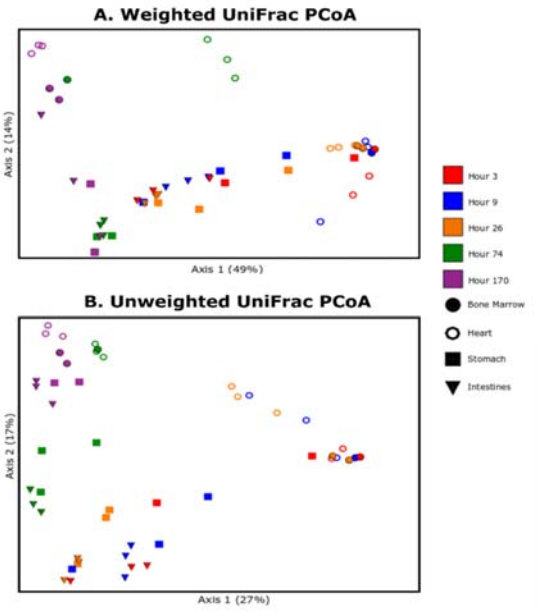

Figure 7. PCoA Plots of mouse organ microbiomes over the postmortem interval for **A.** weighted and **B.** unweighted UniFrac distances. Colors represent the postmortem intervals and shapes represent the organ from where the sample was obtained. Image was created using QIIME 2 and Emperor.

moved the furthest distance on axis 1. The unweighted UniFrac PCoA (Figure 7B) again showed early (≤26h) communities in the heart and bone marrow to be similar but unique from early intestines and stomach with the exception of one 3h stomach sample. As decomposition progressed, both clusters moved across axis 1 (27%) and 2 (17%) until converging. The intestines and stomach communities transition in a "step-like" pattern while the heart and bone marrow transitioned rapidly at 74h. ANCOM determined the differentially abundant taxa over the course of decomposition to be Lactobacillaceae (*W* = 9) and Clostridiaceae I (*W* = 8) in the bone marrow; Lactobacillaceae (*W* = 42), Clostridiaceae I (*W* = 42), and Enterobacteriaceae (*W* = 40) in the heart; Lactobacillaceae (*W* = 47), Enterococcaceae (*W* = 43), and Clostridiales Family XI (*W* = 41) in the intestines; and Clostridiaceae I (*W* = 47) in the stomach.

Following these initial experiments, heart, bone marrow and intestines-associated microbial RNA were subjected to shotgun metatranscriptome sequencing. The edgeR mean transcript library sizes after filtering for the intestines was 8,760.4 (min = 1,138, max = 34,656, SD = 8,760.4), heart was 34,171 (min = 5,717, max = 116,326, SD = 36,751.99), bone marrow was 7,489.47 (min = 2,347, max = 17,850, SD = 5,048.7), and stomach was 14,198.2 (min = 1,448, max = 96,625, SD = 26,168.53). The DESeq2 mean transcript library sizes after filtering for the intestines was 7,019 (min = 1,045, max = 26,751, SD = 8,792.68), heart was 31,480 (min

This resource was prepared by the author(s) using Federal funds provided by the U.S. Department of Justice. Opinions or points of view expressed are those of the author(s) and do not necessarily reflect the official position or policies of the U.S. Department of Justice.

= 5,492, max = 104,198, SD = 33,544.22), bone marrow was 6,722 (min = 2,193, max = 14,501, SD = 4,267.12), and stomach was 12,828 (min = 1,319, max = 87,270, SD = 23,682.44). Significantly differentially expressed transcripts for each method were determined, but only

Organ	Time Comparison	# of significant up-regulated transcripts		# of non-significantly expressed transcripts		# of significant down-regulated transcripts	
		DESeq2	EdgeR	DESeq2	EdgeR	DESeq2	EdgeR
Intestines	Early v. Middle	0(0)	42(0)	15,647	9,642	0(0)	0(0)
	Middle v. Late	0(0)	2,134(0)	15,647	7,470	0(0)	62(0)
	Early v. Late	0(0)	3,684(0)	15,647	5,977	0(0)	5(0)
Heart	Early v. Middle	276(0)	0(0)	19,917	12,945	6(0)	0(0)
	Middle v. Late	1,056(1,023)	7,073(1,023)	19,138	5,859	5(2)	13(2)
	Early v. Late	1,056(1,028)	8,256(1,028)	19,137	4,622	6(4)	67(4)
Bone Marrow	Early v. Middle	0(0)	18(0)	9,949	3,967	0(0)	3(0)
	Middle v. Late	0(0)	45(0)	9,949	3,861	0(0)	82(0)
	Early v. Late	0(0)	32(0)	9,949	3,911	0(0)	45(0)
Stomach	Early v. Middle	0(0)	432(0)	14,300	8,771	0(0)	28(0)
	Middle v. Late	0(0)	1(0)	14,300	8,800	0(0)	430(0)
	Early v. Late	0(0)	0(0)	14,300	9,212	0(0)	19(0)

Table 1. Number of transcripts detected from differential expression analysis. Time comparisons are separated by their postmortem time groups: early (3H,9h), middle (26H,72H), and late (170H). The number of significant transcripts from each analysis method is shown with the number of common transcripts between the two methods in parentheses.

transcripts that were reported as significant by both edgeR and DESeq2 were considered significant in the study (Table 1). Neither the intestines, bone marrow, nor stomach contained significantly up-regulated or down-regulated transcripts from both programs. In total, the heart contained 2,051 significantly up-regulated transcripts and 6 significantly down-regulated transcripts. The significant comparisons came from comparison expression levels between early and late decomposition and comparing middle and late decomposition. The early v. late comparison contained 1,028 up-regulated transcripts with 252 of them being annotated as hypothetical, ribosomal, or unknown and 4 down-regulated transcripts all annotated as hypothetical. The middle v. late comparison contained 1,023 up-regulated transcripts with 247 of them being annotated as hypothetical, ribosomal, or unknown and 2 down-regulated transcripts

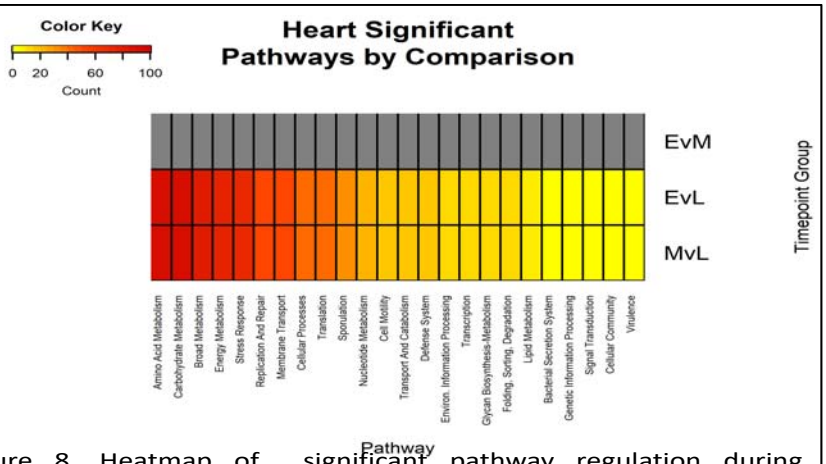

Figure 8. Heatmap of significant pathway regulation during timepoint group comparisons in heart samples. The heatmap represents transcript count of each pathway annotated from the significant transcripts of each comparison by color. Pathway is included on the x-axis and timepoint group (EvL=early v. late, MvL=middle v. late) on the y-axis. Pathways that were not detected in a comparison are gray.

both having a hypothetical annotation. Out of the up-regulated transcripts, 1,022 (99.8%) were shared between the two group comparisons. The most up-regulated pathways were amino acid and carbohydrate metabolism (Figure 8). Other notable pathways include stress response, membrane transport, sporulation, and cell motility.

Over all, we found that known antemortem colonized sites and presumed sterile sites are unique in their colonization patterns. We also provide one of the first analyses into the functional pathways used by bacterial communities colonizing the heart during the decomposing as a first step to discovering post-mortem interval functional biomarkers. These data are very exciting, and suggest the possibility of identifying candidate biomarkers in human samples, as well as validating previously identified candidates across PMI, geography, and body attributes.Overall resulting data from this project also provide rationale for targeting commensal indicator taxa for further, targeted biomarker verification and validation. This approach should provide a more streamlined method for validation of indicators across bodies with diversity across spatial and temporal scales.

Dissemination to communities of interest.

PI Jordan, co-PI Benbow, Dr. Schmidt, Dr. Pechal, and associated students have presented project data at the NIJ R&D meeting 2016 and 2017, as well as at the American Academy of Forensic Sciences meeting 2015-2018. PI Jordan, co-PI Benbow,d and Dr. Schmidt Pechal also

moderated sessions and led discussions on the next steps for forensic science, as well as led a workshop at the 2017 AAFS meeting. PI Jordan, co-PI Benbow, Dr. Schmidt, and Dr. Pechal have presented project preliminary and published data during multiple university seminars throughout the course of this project. Additionally, we have developed a website (https://hpmmdatabase.wixsite.com/hpmmdatabase) to disseminate results of our project including sample numbers, case number, demographic summaries, and list of publications/presentations resulting from this project. Scientists, forensic practitioners, and the general public are anticipated to be able to understand and potentially use the data presented. Further, this funded project opportunity has allow us to expand our network of colleagues to further explore the human post-mortem microbiome.

PI Jordan and Co-PI Benbow several times by phone, email, and in person with local, state and international medical examiners for expansion of sampling methodology and geographical location. Though not part of the current proposal, these collaborations could lead to future studies to expand the geographical range and demographics of cadaver swabs for a broader analysis of the post-mortem microbiome.

Furthermore, PI Jordan also developed and successfully taught a split-level (upper division undergraduate/graduate students) course entitled: “Forensic Microbiology” to 32 students (9 graduate, and 23 undergraduate students). The course content included basic microbiological concepts (section 1), forensically related microbiology studies associated with decomposition, post-mortem interval, cause of death, manner of death, collecting evidence, etc. During the course, PI Jordan also provided information regarding her NIJ funded laboratory experiments. This resulted in an undergraduate volunteer who is now interested in pursuing a career in forensic science.

Impact

Impact of the project on the criminal justice system.

Methods outlined and data obtained from this project are the first to determine how commensal bacterial populations in human remains translocate and proliferate following death with robust statistical power. These data will potentially further investigations and contribute to crime laboratories by identifying specific microbial taxa or metabolic signatures for potential use in quantifiable, precise measurements of PMI used in forensic science. This would also impact the court system as evidence derived from this process could affect prosecution, exoneration of defendants and justice for victims. Additionally, methods for cadaver swabbing and sample collection have been written and disseminated to crime scene investigators at the Wayne County Medical Examiner's office and training has been conducted for standardized sample collection.